PECULARITIES OF THE TEMPERATURE FIELDS IN OXIDE SEMITRANSPARENT CRYSTALS GROWN BY CZOCHRALSKI TECHNIQUE.

O.N.Budenkova [a], V.S.Yuferev [a], M.G.Vasiliev [a] V.V.Kalaev [b].

Ioffe Physico-Technical Institute, 194021 St. Petersburg, Russia

[b] Softimpact Ltd., 194156 St. Petersburg, Russia

Introduction.

Many of oxide dielectrical crystals are semitransparent in the infrared spectrum region at high temperatures. Therefore, during their growth:

- Heat transfer through the crystals is highly intensified by internal radiation.
- Depending on the value of absorption coefficients of the crystal, the radiative thermal sources can influence on temperature field in a crystal to a greater or a lesser extent.

These two facts are well known for objects bounded with *opaque* surfaces. However, the effect of internal radiative heat transfer becomes much more complicated in the case of Fresnel reflection (refraction) of radiation at the crystal side surface. For example, as it was found in Ref.[1], Fresnel reflection causes strong irregularities of temperature fields in $Bi_{12}GeO_{20}$ crystal, whereas in $Bi_4Ge_3O_{12}$ the similar effect is absent (Ref.[2]).

1.O.N.Budenkova, M.G.Vasiliev, V.S.Yuferev, et al, J. of Crystal Growth 266 (2004) 92

2. V.S.Yuferev, O.N.Budenkova, M.G.Vasiliev, et al, J. Crystal Growth 253 (2003) 383.

The aim of the present paper is

to study numerically the special features of temperature fields in oxide semitransparent crystals depending on their thermophysical and optical properties and parameters of growth processes.

Dimensionless parameters

1. **Optical thickness** characterizes the transparency of the crystal

$$\tau = \alpha R$$

α – absorption coefficient in the most transparent range
R – crystal radius (probably, is not the best parameter)

2. **Radiative-conductive parameter** characterizes the relation between the conductive and radiative heat fluxes.

$$M = \kappa_S \alpha / (4n^2 \sigma T_m^3 \tau^2 W_1)$$

T_m – melting temperatures
n – index of refraction
κ_S – thermal conductivity
σ – Stefan-Boltzman's constant
W_1 – Plank's weight function for the most transparent band.

Crystals under consideration:

$Bi_4Ge_3O_{12}$ (BGO-eulithine), Al_2O_3 (α-sapphire), Bi_4GeO_{20} (BGO-sillenite), Bi_4SiO_{20} (BSO-sillenite)

These crystals were chosen for the following reasons:

1. All these crystals are grown by Cz technique;
2. Spectral dependences of their absorption coefficients are known at least at room temperatures;
3. Thermal properties of the crystals are rather different, therefore, variations of τ and M in a wide range can be considered.

Scheme of the calculation domain.

Temperature distributions are given over the crucible wall (line ABCDE) as a boundary conditions

One can expect that:

- the smaller value of τ corresponds to a larger deflection of the solid/liquid interface;
- the smaller is the value of M, the greater is the effect of radiative transport on the internal temperature fields.

Part I.
$Bi_4Ge_3O_{12}$ and Al_2O_3 at:
• close geometrical parameters
• similar boundary conditions relatively their melting temperatures and
• rather different τ and M

$Bi_4Ge_3O_{12}$

Three band approximation of the spectral dependence of absorption coefficient:

λ, μm	κ_S, cm^{-1}	Planck's weight functions
0.5 ÷ 4.0	0.03	W_1=0.6685
4.0 ÷ 6.0	0.9546	W_2= 0.1853
> 6.0	∞	W_3= 0.1462

$R_{Crystal}$= 3.85 cm
M=0.15
τ = 0.116

Typical temperature field and the shape of the SLI for diffusely reflecting conical crystal surface:

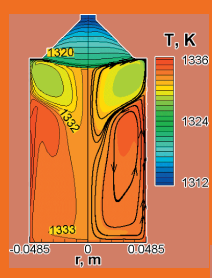

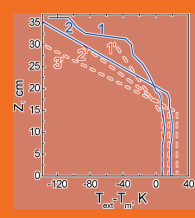

Fig.1. Temperature distributions over the crucible wall:

1, 2 – BGO-eulithine crystal
1′,2′,3′ – Al_2O_3 crystal

Variations in radial temperature in sections AA for different external gradients

BGO-eulithine

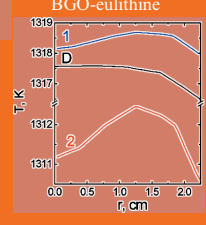

Sapphire

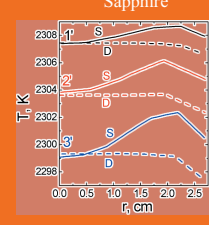

Temperature fields obtained for curves 1 and 2 (Fig.1) for specularly reflecting crystal surface.

external gradient increases

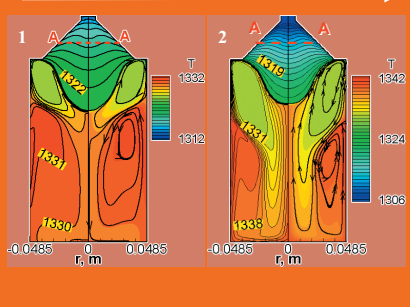

1. Deflection of the SLI in BGO-eulithine crystal is much more greater then in Al_2O_3 both for diffusely and specularly reflecting conical surface (because of smaller value of τ);
2. Peculiarities in temperature fields ($M|_{sapphire} < M|_{BGO}$):
2.1. Radial non-uniformity of temperature fields is greater in sapphire crystal than in eulithine one.
2.2. When increasing external temperature gradient (increase the crystal cooling):
   - in sapphire crystal the center of the boule is cooled more intensively than the crystal surface;
   - in BGO-eulithine temperature of the whole crystal decreases.

Sapphire (Al_2O_3)

Three band approximation of the spectral dependence of absorption coefficient:

λ, μm	κ_S, cm^{-1}	Planck's weight functions
0.5 ÷ 4.0	0.1926	W_1 = 0.8834
4.0 ÷ 4.5	2.5460	W_2 = 0.0280
> 4.5	∞	W_3 = 0.0886

$R_{Crystal}$= 5.5 cm
$M = 8.1 \cdot 10^{-3}$
τ = 1.05

Typical temperature field and shape of the SLI for diffusely reflecting conical crystal surface.

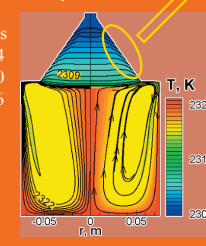

The bend of isotherms is related to the crystal cooling directly from its surface due to the opaque band in spectrum of absorption coefficient.

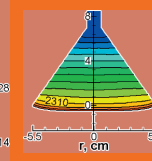

Temperature field in the crystal calculated for the case W_3=0.0

Temperature fields obtained for curves 1'-3' (Fig.1) for specularly reflecting crystal surface.

external gradient decreases

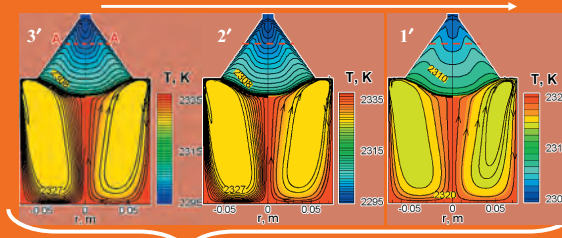

Temperature fall in the crystal center is not conditioned by the convexity of the crystallization front since it can be observed for the flat interface as well !

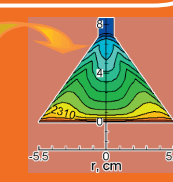

Part II:
$Bi_{12}SiO_{20}$ and $Bi_{12}GeO_{20}$ at:
• the same geometrical parameters
• similar boundary conditions relatively their melting temperatures and rather different τ and M

$Bi_{12}SiO_{20}$

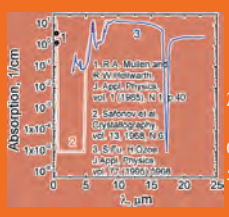

Three band approximation of the spectral dependence of absorption coefficient:

λ, μm	κ_S, cm^{-1}	Planck's weight functions
0.5 ÷ 5.1	0.1019	0.7823
5.1 ÷ 7.5	3.4705	0.1248
> 7.5	∞	0.1249

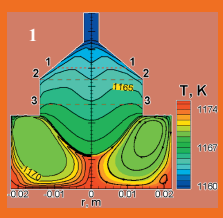

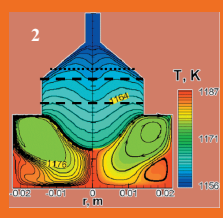

$R_{Crystal}$= 1.4 cm

$M = 4.8 \cdot 10^{-2}$
τ = 0.1426

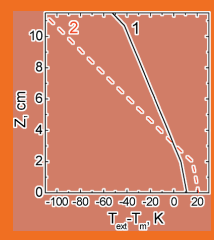

Fig.1. Temperature distributions over the crucible wall

(the same for both crystals)

$Bi_{12}GeO_{20}$

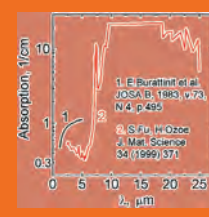

Three band approximation of the spectral dependence of absorption coefficient:

λ, μm	κ_S, cm^{-1}	Planck's weight functions
0.0 ÷ 6.89	0.482	0.8672
6.89 ÷ 9.16	5.983	0.0649
> 9.16	∞	0.0679

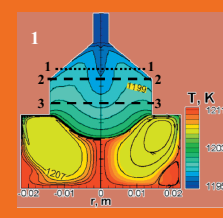

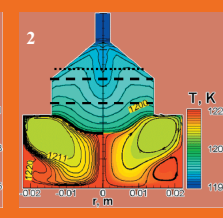

Variations in radial temperature at specified heights for different external gradients.

Section 1-1

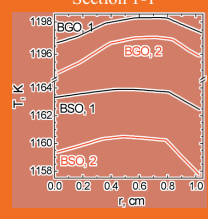

Section 2-2

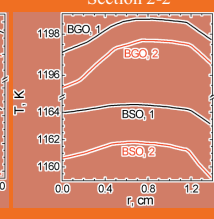

Section 3-3

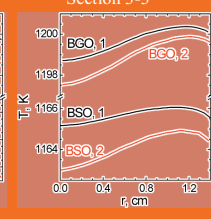

$R_{Crystal}$= 1.4 cm
$M = 9.99 \cdot 10^{-3}$
τ = 0.6758

1. Deflection of the SLI in BSO-sillenite crystal is slightly greater then in BSO-sillenite (because of smaller value of τ);
2. Concerning temperature fields ($M|_{BSO} > M|_{BGO}$):
2.1. Radial non-uniformity of temperature fields is greater in BGO-sillenite crystal than in BSO-sillenite one.
2.2. Increasing of external temperature affects on the temperature distributions in these crystals differently:
   - in BGO-sillenite crystal the center of the boule is cooled more intensively than the crystal surface;
   - in BSO-sillenite crystal temperature of the whole crystal decreases.

Growth parameters and materials properties

	Al_2O_3	$Bi_4Ge_{12}O_3$	$Bi_{12}GeO_{20}$	$Bi_{12}SiO_{20}$
Growth parameters				
Melting temperature, K	2313	1323	1203	1168
Crystal/crucible radius, cm	5.5 / 7.5	3.85 / 4.85	1.4 / 2.2	1.4 / 2.2
Crystal rotation rate, rpm	35	35-15	15	15
Pulling rate, mm per hour	7	5	10	10
Crystal properties				
Absorption coefficient of the crystal in the most transparent band, cm^{-1}	**0.1926**	**0.03**	**0.4822**	**0.1019**
Index of refraction	1.78	2.15	2.36	2.54
Thermal conductivity, W/(m·K)	3.0	1.2	0.18	0.18
Radiative-conductive parameter M	**$8.1 \cdot 10^{-3}$**	**0.15**	**$9.99 \cdot 10^{-3}$**	**$4.8 \cdot 10^{-2}$**
Melt properties				
Density, kg/m^3	3100	6710	8130	7630
Kinematical viscosity, m^2/s	$1.51 \cdot 10^{-5}$	$6.17 \cdot 10^{-6}$	$2.09 \cdot 10^{-6}$	$2.88 \cdot 10^{-6}$
Thermal conductivity, W/(m·K)	3.5	0.7832	0.345	0.345
Specific heat, J/(kg·K)	1300	356	390	390
Expansion coefficient, 1/K	$3 \cdot 10^{-5}$	$7.6 \cdot 10^{-5}$	$1.2 \cdot 10^{-4}$	$1.2 \cdot 10^{-4}$

Conclusions

Results presented here demonstrate the extremely important role of specular reflection in formation of the temperature fields in oxide crystals grown by Cz technique.

1. Specular reflection at the side surface of crystals can results in strong distortion of isotherms in crystalline phase.
2. Distortion of temperature isolines correlates with the magnitude of conductive-radiative parameter: the less is value M, the greater distortion of temperature field one should expect.
   2.1. There should be non-uniform dependence of temperature perturbation on the value M, since M=0 corresponds to opaque crystals
3. Deflection of the crystallization front depends on the optical thickness in the same way: the less is the optical thickness, the greater is the convexity of the SLI.
4. Resulting temperature distribution depends on both internal and surface radiation and, therefore, multiband models have to be used for simulation.